DEVELOPMENTAL BIOLOGY **173,** 133–147 (1996)
Article No. 0012

Immigration and Ventral Sprouting of Endothelial Cells

Haymo Kurz,* Torsten Gärtner,* Peter S. Eggli,† and Bodo Christ*

**Anatomisches Institut II, Albert-Ludwigs-Universität Freiburg, Albertstrasse 17, D-79104 Freiburg, Germany; and †Anatomisches Institut, Universität Bern, Bühlstrasse 26, CH-3000 Bern 9, Switzerland*

We studied the early pattern of neural tube (NT) vascularization in quail embryos and chick–quail chimeras. Angioblasts appeared first in the dorsal third at Hamburger and Hamilton (HH) stage 19 as single, migrating cells. Their distribution did not correspond to a segmental pattern. After this initial dorsal immigration, endothelial sprouts invaded the NT on either side of the floor plate (HH stage 21). These cells remained continuous with their arterial vascular sources, connected to the venous perineural vascular plexus at HH-stage 22, and formed the first perfused vessels of the NT at HH-stage 23. The same pattern of angiotrophic vascularization was observed in a craniocaudal sequence starting caudal to the rhombencephalic NT. Extremely long filopodia were observed on sprouting cells, extending toward the central canal and the mantle layer. The exclusively extraneuroectodermal origin of angioblastic cells was demonstrated with chick–quail chimeras. Following replacement of quail NT by chick NT graft, angioblast and sprout distribution in chimeras was the same as in controls. We conclude that the NT receives its first blood vessels by a combination of two different processes, dorsal immigration of isolated migrating angioblastic cells and ventral sprouting of endothelial cells, which derive from perfused vessels. The dorsal invasive angioblasts contribute to the developing intraneural vascular plexus after having traversed the neural tube. The initial distribution of blood vessels within the neuroepithelium corresponds to intrinsic random motility of angioblastic cells; a more regular pattern is seen later. The floor plate apparently prohibits connections between sprouts in both NT sides, whereas in the dorsal NT, such a separating effect on the migrating angioblasts does not exist.

INTRODUCTION

The classic study on the development of the intraneural blood vessels in avian embryos is the report by Feeney and Watterson (1946). They described the first appearance of intraneural capillaries in specific regions of the neural tube (NT) periphery, in a definite sequence, and with a definite course internally, altogether resembling a nonrandom pattern. Strong (1961) also stressed ''that the control of position of each capillary is very precise.'' Concerning the actual mechanism of NT vascularization, however, he was quite at variance with Feeney and Watterson (1946) and with earlier observations by himself (Strong and Winston, 1957). He no longer favored sprouting into the NT, but intraneural development of ''solenomorphic'' cell cords into a plexus, which only later should connect to perineural vessels. All of these studies, including that by Camosso *et al.* (1976), had relied on conventional histology in combination with india ink injections and, therefore, could detect only patent and perfused vessels with certainty, whereas the putative angioblastic nature of mesenchymal masses within the neural tube, or their origin, could not be established.

Studying craniofacial blood vessel development with quail–chick transplantation experiments, Noden (1991) concluded that, in spite of the extensive migratory capability of blood vessel progenitors, only sprouts, but no invasive angioblasts, entered the neural epithelium. This is in concordance with a recent study on the angiogenic potential of the somite (Wilting *et al.*, 1995a), which demonstrated that endothelial cells contribute to patent blood vessels in the

0012-1606/96 $12.00

neural tube at the sixth day of development. Our first observations, however, indicated the presence of invasive angioblasts in early 4-day embryos. This prompted us to initiate this study on a series of normal stages of quail embryos, and in chick–quail chimeras, with the monoclonal antibody QH1 (Pardanaud *et al.*, 1987), directed against quail angioblasts and endothelial cells. Here, we use a combination of 3-D reconstructions, confocal laser scanning microscopy, and spatial statistics to describe the three-dimensional distribution and shape of angioblastic cells in the avian neural tube during the fourth day of development.

MATERIALS AND METHODS

Embryos, Fixatives, and Sectioning

Quail (*Coturnix coturnix japonica*) embryos were incubated for 72 to 96 hr at 311 K and 75% humidity. After fenestration of the shell, they were quickly cut off the yolk, rinsed in cold phosphate-buffered saline (PBS), pH 7.4, staged according to Hamburger and Hamilton (1950, referred to as HH stage), and sacrificed in a solution of 97% ethanol and 3% acetic acid. Specimens were prepared for paraffin embedding after their heads were removed cranial to the hindbrain. Transverse serial sections of 5 μm were cut such that sequences of 150 to 200 sections were obtained, which immediately followed the caudal end of the rhombencephalic NT region. Additional embryos of HH-stages 23 and 27 were sacrificed in Serra's fixative (60% ethanol, 10% formalin, 10% acetic acid) for 7 hr and rinsed in PBS for 24 hr at 277 K. They were then embedded in 5% agar agar (Merck, Darmstadt, Germany) and cut on a vibratome (Leica, Bensheim, Germany) at 100-μm thickness. Slices were transferred to 24-microwell plates for further processing at room temperature on a tumbler.

Paraffin Section Immunocytochemistry

Sections were dewaxed in Rotihistol (Roth, Karlsruhe, Germany) and through a graded series of alcohols. Endogeneous peroxidase was blocked with 0.03% H_2O_2 in methanol for 30 min at 310 K. All further steps were carried out at room temperature. Rinsing in PBS plus Tween was followed by two washes with PBS. Preincubation with 1% BSA for 20 min prevented unspecific binding of the primary monoclonal antibody QH1 (Dakopatts, Hamburg, Germany, raised in the mouse), which was applied at a concentration of 1:1500 for 90 min. After two washes with PBS, the secondary peroxidase-coupled antibody (Sigma, Deisenhofen, Germany, raised in the goat), was applied at a concentration of 1:250 for 90 min. The nickel-intensified 3,3′-diaminobenzidine tetra-hydrochloride (DAB) reaction for peroxidase activity demonstrated the QH1-positive structures. After shortly counterstaining with nuclear red, and following dehydration, slides were sealed with coverslips and Rotihistokitt (Roth).

Vibratome Slice Immunocytochemistry

Slices were treated with 0.4 % Triton X-100 in PBS for 24 hr, preincubated for 2 hr with 0.2% Triton plus 1% BSA, and incubated with QH1 (1:1000) for 20 hr. After four washes with PBS plus 0.2% Triton within 1 hr, the secondary Cy3-coupled antibody (Dianova, Hamburg) was applied for 14 hr. Following four final washes with PBS within 2 hr, sections were mounted under coverslips with Mowiol (Hoechst, Germany). On either side of the mounted slice, a small coverslip of 150-μm thickness was inserted to avoid compression.

Controls and Histochemistry

Additional series of dewaxed sections were treated with the DAB reaction alone, as described above but without blocking endogeneous peroxidase, or without the first or second antibody to detect unspecific staining or endogenous myeloperoxidase activity (MPX). For the detection of macrophages, an unspecific esterase reaction was performed on additional samples with a ready-made kit (Sigma, Deisenhofen, Germany) as prescribed by the manufacturer.

Chick-Quail Chimeras

Chick embryos (HH-stages 12–14) served as donors of neural tube pieces of approximately 500 μm in length, and quail embryos (HH-stages 12–15) as hosts. The chick donor was dissected from the yolk and transferred to a petri dish filled with Locke's solution. The embryo was affixed to the agar bottom layer of the dish, and the neural tube was prepared in the region of the most caudal somites such that a tiny piece of the notochord remained at its cranial end. The NT was then transferred to a solution containing 0.4% trypsin to digest adherent cells. After approximately 4 min, the NT was put in horse serum to stop the enzymatic reaction.

Simultaneously, the quail host's neural tube was removed *in ovo* at a corresponding position and length. The graft was transferred to the quail egg with a Spemann pipette and was inserted into the host in normal orientation. The amnion was closed, and the fenestrated egg shell was sealed with tape. The operated hosts survived until HH-stage 23 and were fixed in Serra's fixative. Four successful grafts were evaluated. In addition, the transplantation was performed *vice versa*, with quail donor and chick host. Three succesful grafts were evaluated.

Image Analysis and 3-D Reconstructions

A Zeiss (Oberkochen) standard microscope, equipped with 16X and 10X objectives, was connected to a black and

white CCD camera (Hitachi). Green light of 564 nm was used for contrast enhancement. The video signal was digitized with a framegrabber (Matrox/Canada: PIP 1024B, 512 × 512 pixel, 8 bit gray value resolution) in a Pentium PC, which was operated with the image analysis package analySIS 2.0 and the 3-D reconstruction package 3DSIS (SIS, Münster, Germany). Up to 70 serial sections of HH-stages 19, 21, and 23 embryos were used for 3-D reconstructions. The long axis of the ellipsoidal central canal served as the *y*-axis. A line from the center of the circular notochord and perpendicular to the *y*-axis was defined as *x*. With the notochord as the natural *z*-axis, section alignment posed no serious problems, and only minor adjustments for rotational or translational deviation were necessary.

Microscopy, Confocal Laser Scanning Microscopy, and Photography

A Zeiss Axioskop microscope with PlanNeofluar ×10, ×20, and ×40 was used for microphotography of microtome sections with green light (564 nm) on AgfaOrtho 25 film material. Vibratome slices of 100-μm thickness were imaged with the Bio-Rad MRC-600 confocal laser scanning microscope equipped with a krypton/argon mixed gas laser. The K1/K2 filter set was employed for Cy-3 fluorescence. A Nikon microscope with 10X (CF PlanApochromat, aperture 0.45) and 40X (CF Fluor Oil, aperture 1.3) objectives was used. The pinhole aperture was maintained as small as was commensurate with an adequate signal intensity. Up to 60 serial optical sections were produced at 2-μm (×10) or 1-μm (×40) intervals. Digitized images of each optical plane were Kalman-averaged and further processed using Bio-Rad CoMOS software. Pictures of superimposed optical sections were taken from a Polaroid FreezeFrame video recorder using Agfa APX 100 film material.

Quantitative Evaluation

QH1-positive cells were identified and counted in complete serial sections, and for the left and right NT half separately. Lateral differences in cell number were compared with a χ^2 test at a significance level of $P < 0.05$.

The problem of analyzing the three-dimensional distribution of QH1-positive cells (angioblasts or sprouts) in serial sections was split into three one-dimensional problems: (1) the lateromedial position of cell centers was measured on the shortest line between the basal lamina of the neuroepithelium and the surface of the central canal and expressed in relative units; (2) the dorsoventral positions of angioblasts were classified as located in the dorsal, intermediate, or ventral NT third; (3) the craniocaudal distribution of angioblasts was assessed as nearest-neighbor-distances between the cell centers, in multiples of section thickness, and in any of the dorsoventral thirds separately. All three analyses were carried out for both sides of the NT separately, for at least 150 subsequent sections, and for two embryos of each HH-stage 18 through 24. It should be noted that all measures were in relative units and therefore did not depend on (possibly nonuniform) shrinkage during tissue preparation.

From the mean distance d between angioblastic cells, the parameter λ of a Poisson distribution was estimated as

$$\lambda = \frac{1}{2d}; \quad F(x) = 1 - e^{-2\lambda x}.$$

The observed distribution was then compared with the calculated Poisson distribution applying the Kolmogoroff–Smirnov test to $F(x)$ at a significance level of $P < 0.05$. For detailed information on spatial statistics refer to Stoyan and Stoyan (1994).

RESULTS

QH1 Immunohistochemistry

The typical appearance of cervical sections from quail embryos at HH-stages 20, 21, and 23 following QH1 immunohistochemistry is shown in Fig. 1. Single angioblasts and differentiated endothelial cells show the black QH1 signal. Until HH-stage 20, the neural tube is supplied with nutrients exclusively from outside via dorsal segmental branches of the aorta, which connect to the primitive arterial tract (PAT, Sterzi, 1904) on either side of the floor plate. The blood then flows through the perineural vascular plexus (PNVP) lateral to the NT and drains toward the cardinal veins. This traditional view, as summarized by Camosso *et al.* (1976), was fully confirmed by QH1 staining of endothelial cells in patent vessels and by earlier ink injection experiments (data not shown). Our subsequent description will focus on angiogenetic processes in the neuroepithelium.

At HH-stage 20, the first QH1-positive cells were seen in the dorsal third of the NT (Fig. 1A), but may appear as early as HH-stage 19 (approximately 72 hr incubation). On single sections, these cells appeared with circular or flat ellipsoidal cross sections and with single lamellipodia. The largest cell diameter observed was almost 100 μm, with the cell extending from the mantle to the ependymal layer.

At HH-stage 21, multiple angioblast profiles could be found in a single section, most often located near the site of dorsal root formation (Fig. 1B). First sprouts were observed penetrating the NT basal lamina between floor plate and basal plate and originating from the PATs. Until HH-stage 22, these sprouts were confined to the ventral third of the NT and were never seen invading the developing motor column.

At HH-stage 23, first continous blood vessels have formed in the ventral third, which take a course around the motor column, connecting the PAT with a ventral portion of the PNVP (Fig. 1C). Until HH-stage 24 (approximately 96 hr incubation), round or elongated angioblasts were seen in

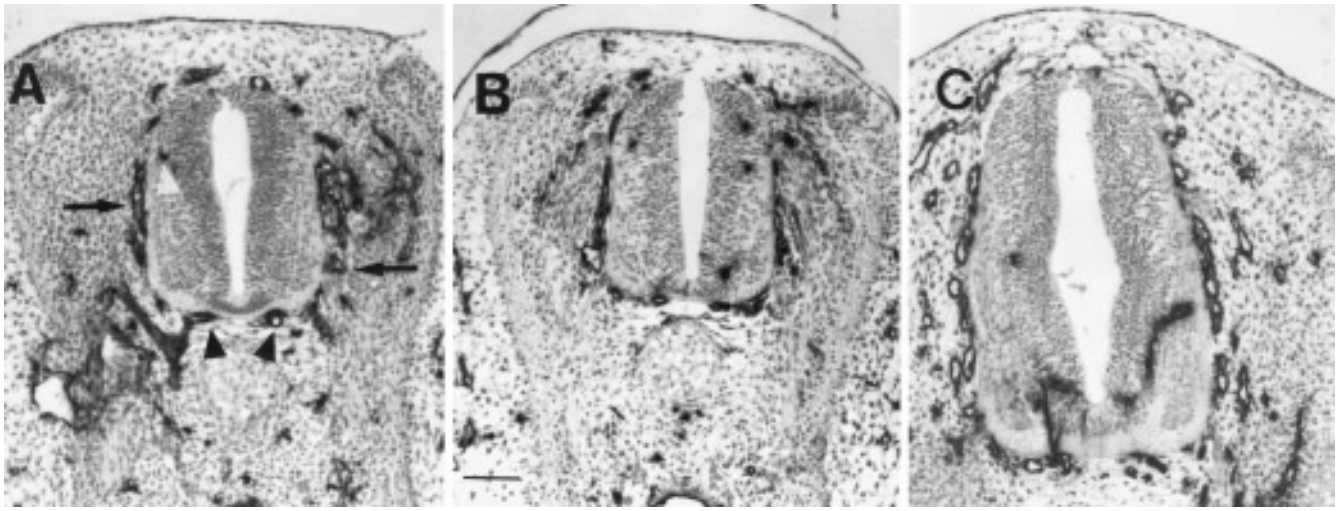

FIG. 1. Cervical portions of quail neural tube (NT) after QH1-immunoperoxidase reaction and nuclear red staining. Angioblasts and endothelial cells appear as black structures with or without a lumen, isolated or connected to patent vessels. Note the densely arranged neuroblast nuclei in the NT ependymal layer. (A) At HH-stage 20, the primitive arterial tracts (PAT, arrowheads) supply the well-developed perineural vascular plexus (PNVP, arrows). The PNVP covers most of the NT circumference but spares the floor and roof plates, where patent vessels are rare. Note one profile of an isolated angioblast in the dorsal third (white arrowhead). (B) At HH-stage 21, more angioblasts are seen in the dorsal and intermediate third of the NT. The tip of a ventral sprout is seen in the right half. (C) At HH-stage 23, ventral sprouts have reached the intermediate NT third, where they will connect to sprouts originating from the PNVP. In addition, sprouts on both sides have reached the central canal, but will fail to form connections in this region. Note the isolated angioblast on the left side. Scale bar, 100 μm.

the dorsal and intermediate third, but only occasionally in the ventral third.

Features common to all stages of the fourth day of development were: (1) angioblasts avoided the ependymal layer with densely packed neuroepithelial nuclei; (2) marked left–right asymmetry of angioblasts or sprouts; (3) lumen formation occurred only in the ventral third.

3-D Reconstructions

Visualization of angioblast distribution in the neural tube was achieved with 3-D reconstructions of up to 70 serial 5-μm sections. Figures 2A–2C show that from the beginning there was a considerable asymmetry over 350 μm, which still persisted in any of the three stages shown (same specimens as in Fig. 1).

At HH-stage 20, angioblasts appeared only in the dorsal third as large, multiform, and unconnected cells (Fig. 2A). The most ventral cells of this group reached a common level on both sides, corresponding approximately to the border between dorsal and intermediate NT third. The well-developed and perfused PATs obviously did not contribute to the intraneural angioblasts population.

At HH-stage 21, sprouts originated from the PATs only in the very well-defined region between the floor plate and the future motor column (Fig. 2B). No bilateral symmetry was observed for the distribution of sprouts nor for dorsal angioblasts, but rather a considerable variability in shape

FIG. 2. Three-dimensional reconstructions of serial sections (same specimens as Fig. 1). Neural tube (NT) and central canal, yellow; notochord, blue; PATs outside, and angioblasts or sprouts inside, the NT, red. The PNVPs are omitted for clarity. Oblique aspects from slightly different angles are shown. (A) At HH-stage 20, most angioblasts are arranged in a region between the dorsal and the intermediate third, with most cells dorsal to this. Elongated shape of angioblasts suggests migratory activity. Note the lateral difference: three cells are on the left, but six cells are on the right side. Sprouts are extremly rare and were not seen in this series of 60 sections (300 μm). (B) At HH-stage 21, the dorsal angioblasts have more irregular shapes and may be found at varying positions in the dorsal or intermediate third. Ventral sprouts have penetrated into the NT, they are spaced at irregular intervals, and appear strongly asymmetrically: four on the left, and only one on the right side. (C) At HH-stage 23, the dorsal and intermediate angioblast population still is present, but ventral sprouts are more numerous. The sprouts have made their way around the developing motor column and have connected to lateral sprouts and formed a patent lumen so that circulation starts. Note the asymmetric angioblast and vessel distribution.

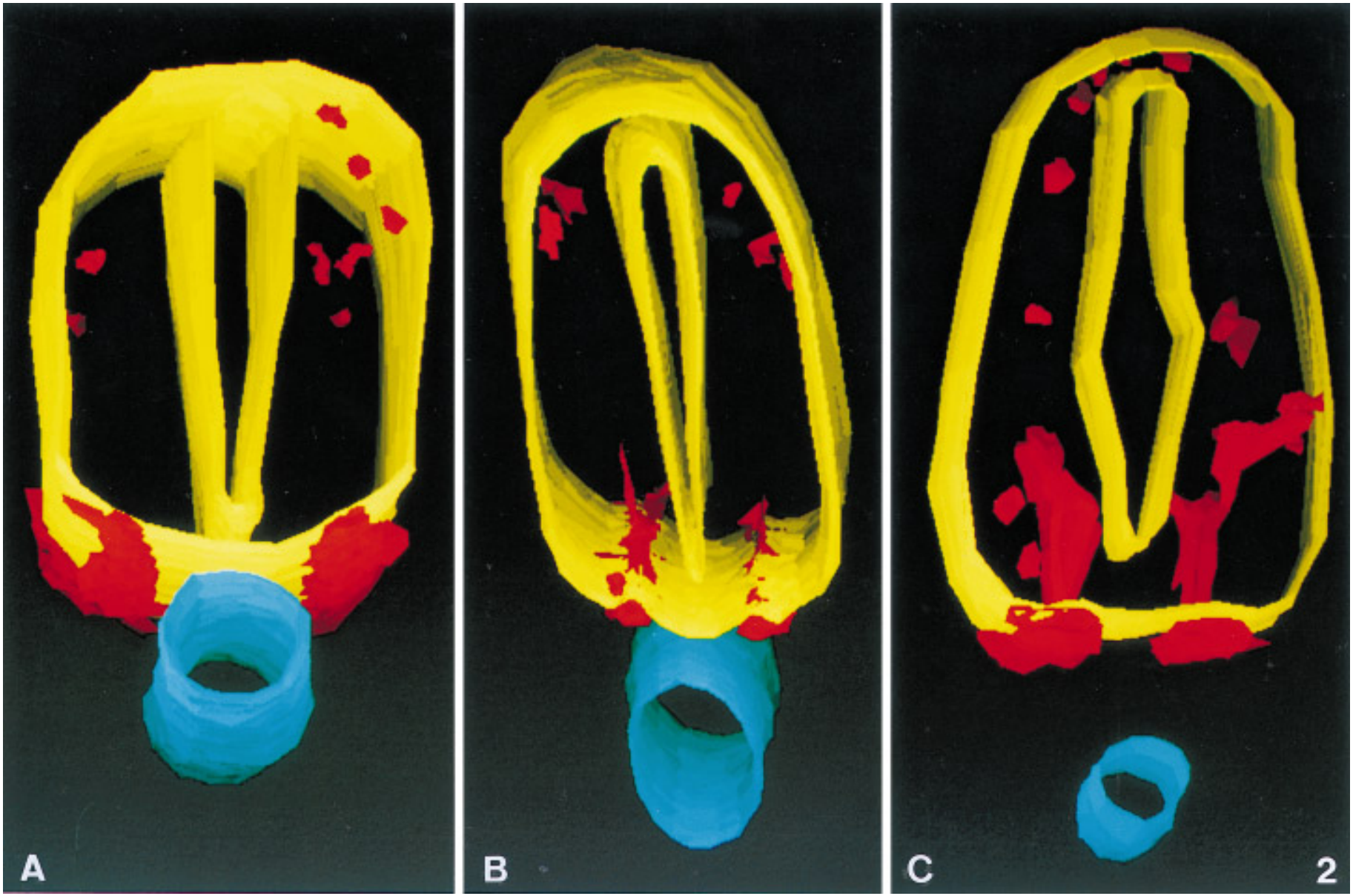
A
B
C
2

and orientation. Some cells had their processes directed toward the central canal, others away from it; sometimes, a fusiform angioblast was found interposed between the developing anterior horn and the NT basal lamina, but still in contact with the PAT. The dorsal third at HH-stage 21 was populated with an increasing number of still larger angioblasts, which began to invade the intermediate third on their ventrad course through the NT. A region without QH1-positive cells was present between the dorsal and the ventral population until HH-stage 22.

At HH-stage 23, the majority of QH1-positive cells was found in the ventral third, forming patent vessels in axial and lateral direction. Here, the first connections with the PNVP were made. Again, some sprouts had their processes directed against the wall of the central canal. While the ventral pattern had become more symmetrical, the distribution of dorsal angioblasts was still asymmetric. No patent vessels were seen in the dorsal NT third until HH 24. Floor plate and motor column remained absolutely free from angioblasts, and both of the PATs of either side and the sprouts inside the NT remained unconnected during the period HH-stage 19 to 24. In contrast, dorsal angioblasts were seen interposed between roof plate cells even in the midline. After HH-stage 23, isolated angioblasts were also seen close to, or associated with, sprouts in the ventral third of the neural tube.

Confocal Laser Scanning Microscopy

The QH1 epitope was detected in thick tissue slices (vibratome sections of 100 μm) with a prolonged permeabilization and immunostaining protocol. We used a Cy3-coupled secondary antibody and obtained a bright, fading-resistant signal through the entire thickness of the slice. The working distance of the microscope objectives was more than 300 μm, which sufficed to scan through the complete specimens without optical distortions. In a HH-stage 23 embryo, the simultaneous occurrence of isolated angioblasts and of sprouts, and the interconnections formed between sprouts, are demonstrated in Fig. 3. In Fig. 4, we show the typical appearance of sprouts with numerous filopodia and the smooth cell surface of an angioblast.

Figure 3A shows that the extraneural vascular pattern, constituted by the somitic segmentation, is quite different from the intraneural sprout distribution. The craniocaudal diameter of the somites here was about 220 μm, whereas sprouts were spaced at intervals varying from 30 to 100 μm. In addition, isolated angioblasts inside the NT were observed, with a shape similar to those of differentiating endothelial cells in the somite-derived connective tissue. The formation of a longitudinal arcade is seen in Fig. 3A, whereas in Fig. 3B, the connection of a ventral with a lateral sprout is shown. Filopodia at the tips of sprouts apparently were essential for establishing the first contact between the leading cells at the tips, whose cell bodies initially were separated by about 100 μm.

Filopodia originating from ventral and lateral sprouts showed a beaded appearance and reached lengths of 50 μm or more (Figs. 4A, 4B). Once the sprout had penetrated into the ventral neuroepithelium, a major portion of filopodia was directed toward the ependymal layer (Fig. 4B). Single filopodia reached the inner surface of the central canal (Fig. 4A). Few filopodia were directed toward the motor column but were never found inside this region. Isolated angioblasts were found in the ventral third between sprouts and were continually present in the more dorsal NT regions. Comparison of HH-stage 23 with stage 27 embryos showed that the vessel formation at other levels of the NT corresponded to that described for the cervical NT level.

Chick–Quail Chimeras

The extraneural origin of angioblastic cells during neural tube vascularization was demonstrated with quail embryos, in which a portion of the NT had been replaced by chick NT at the leg level (Figs. 5, 6). Following transplantation at HH-stage 13 and after reincubation until HH-stage 26, the neural tube was perfectly integrated in the host embryo: neuroblasts in the motor column had formed ventral roots (Fig. 5). Graft-derived neural crest cells had formed dorsal root ganglia, dorsal roots, and Schwann cell precursors (Fig. 6). The blood vessel pattern outside the neural tube was normal, and no signs of malformation or impaired function were observed.

Both angioblasts in the dorsal region and sprouts in the ventral region were QH1-positive, indicating their host origin. Shape and distribution of blood vessel precursor cells paralleled the cervical late HH-stage 22 pattern in normal quail embryos: (1) sprouts between floor plate and motor column had multiple long filopodia (Fig. 5); (2) isolated, flat angioblasts were concentrated close to the dorsal root level but avoided the ependymal layer (Figs. 6A–6C).

Two subsequent serial sections are shown in Figs. 6B and 6C. In Fig. 6B, the continuity of the ventral sprout with the PAT is obvious, whereas in Fig. 6C the sprout processes can be seen. The dorsal angioblast displays a round cell body in Fig. 6B, whereas in Fig. 6C its long, flattened cell process can be seen, which resembles a lamellipodium. This isolated, invasive angioblast is located in immediate proximity to the PNVP at the dorsal root entrance.

Quantitative Evaluation

In 12 complete series of transverse cervical sections (HH-stage 19 through 24), number and position of QH1-positive cells were registered. Hence, an estimate of numerical density and of relative position was achieved, based on three-dimensional information over approximately 1 mm of NT length per specimen.

Bilateral asymmetry. As demonstrated before with 3-D reconstructions, the left and right NT halves did not show bilateral symmetry. In HH-stages younger than 22, one NT half was found to contain, e.g., eight QH1-positive cells,

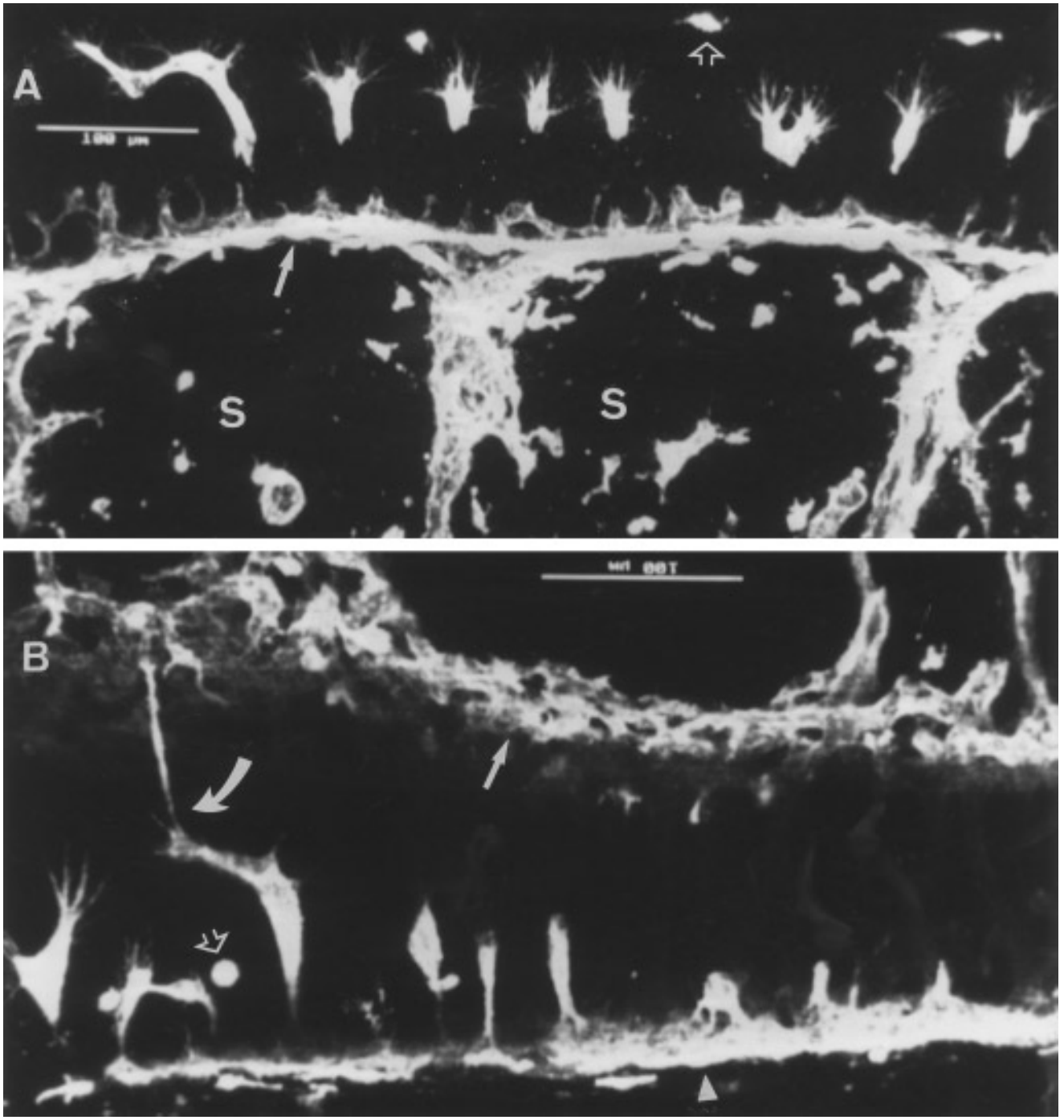

FIG. 3. Confocal laser scanning microscopy (CLSM) of a HH-stage 23 quail stained for QH1. (A) Longitudinal, oblique slice (100 μm) through somite-derived tissue (S) and intermediate third of neural tube (superimposition of 40 optical sections, spaced 1 μm apart). Note the segmental vessels, the perineural vascular plexus (PNVP, arrow), and the differentiating angioblasts in the somite-derived mesenchyme. Inside the NT, a series of sprouts with numerous filopodia can be seen. Their blunt ends indicate the lower face of the physical section. Note longitudinal arcade formation and bifurcations. In the more dorsal part of the slice, three isolated angioblasts can be seen (open arrow). (B) Longitudinal, paramedian slice (100 μm) through ventral and intermediate third of neural tube (superimposition of 14 optical sections). Note the primitive arterial tract (PAT, arrowhead) at the ventral (bottom), and the PNVP (arrow) at the lateral (top) side of the NT. A series of ventral sprouts with variable shape and extension originates from the PAT. A single lateral sprout has connected to filopodia of a ventral half-arcade (curved arrow). Note the isolated angioblast in between the sprouts (open arrow). Scale bars, 100 μm.

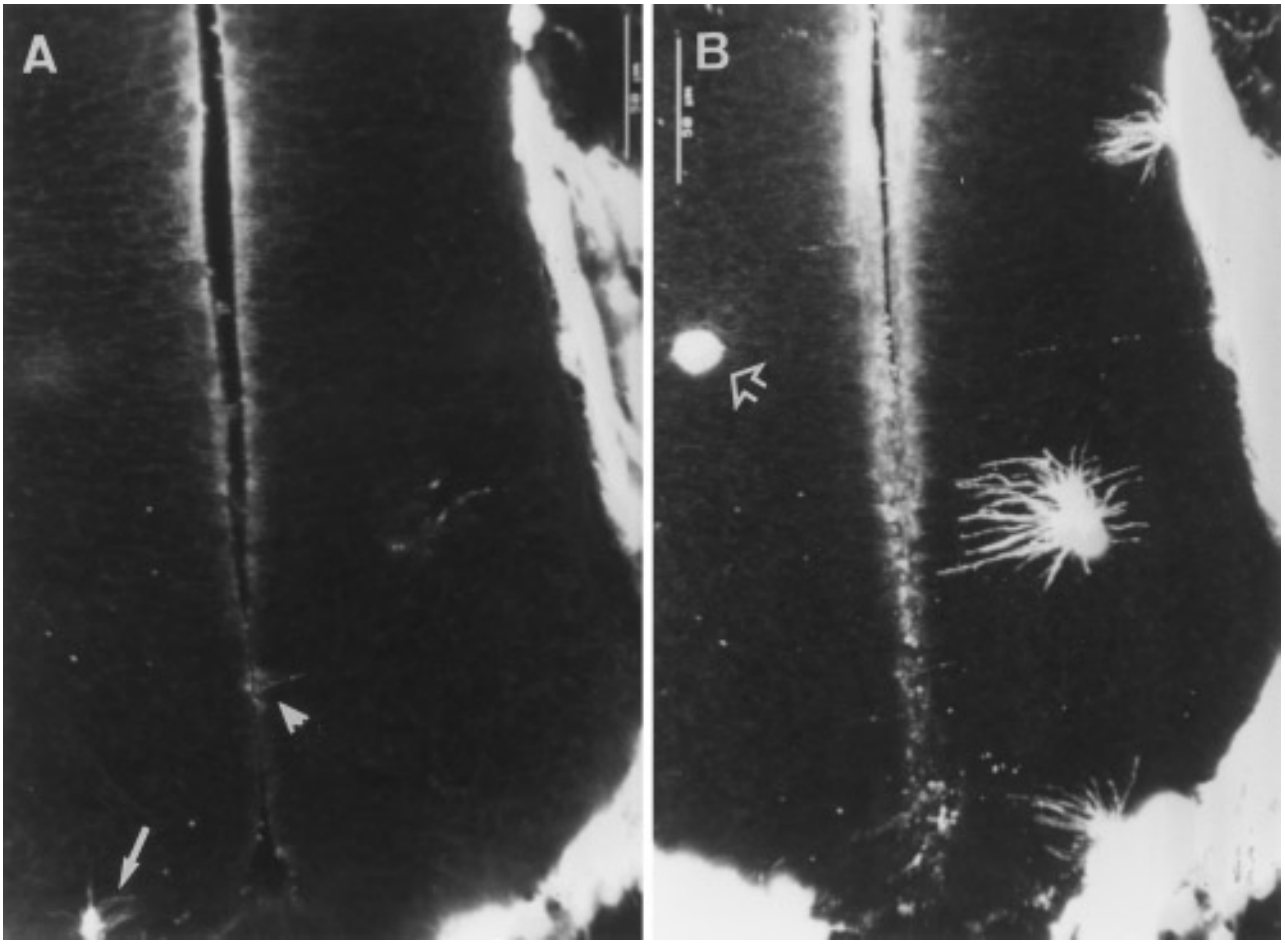

FIG. 4. CLSM of a HH-stage 23 quail neural tube stained for QH1 (transverse slice 100 μm, floor plate and basal plate). (A) Superimposition of the first two optical sections (1 μm apart). Note the minute sprout in the left half (arrow) and the very thin isolated filopodia in the right half, one reaching the ependymal surface (arrowhead). (B) Superimposition of 40 optical sections. In the right half, the large tip of a ventral sprout, a minor ventral, and a lateral sprout show an abundance of long (some longer than 50 μm) filopodia. Note the isolated angioblast (open arrow) in the left half, which was not present in A. Scale bars, 50 μm.

where not a single one could be observed in the other half. This corresponded to a probability of $(0.5)^8 < 0.5\%$. For larger series, and for the combined count of four embryos, however, the left and right number of angioblasts were approximately balanced.

Lateromedial distribution. Measurements of angioblast position from four embryos per age group, and from left and right NT halves, were combined into the histograms of Fig. 7. Note the wide distributions of angioblasts, which have their median value at 30% distance from the basal lamina in HH-stages 19 through 22. In HH-stages 23 and 24, a bimodal distribution was found, with peaks at 40 and 55%. Angioblasts in the NT were not confined to narrow paths; they were spread over a broad range, particularly in the older stages. Nevertheless, the tendency to shift their preferred position toward the ependymal layer is obvious. The inner third, however, was almost completely free of angioblasts. Here the neuroblast nuclei are most densely packed (cf. Figs. 1A–1C, and 6A). The peaks of the distributions corresponded to zones where fewer neuroblast nuclei were found. The pattern of migrating angioblasts was different from that of sprouting endothelial cells, with more cells in the inner third and no cells in the lateral half (motor column).

Dorsoventral distribution. In Fig. 8, the number of angioblasts per 100 μm of NT length, N_L, is shown. Sprouts were included in the count for the ventral third. Obviously, a considerable number of angioblasts populated the neural tube in its dorsal and intermediate third before sprout formation started in the ventral third. While void of angioblasts before HH-stage 21, more than 90% of sections contained QH1-positive structures in the ventral third at HH-stages 23 and 24. The ventral population, consisting of

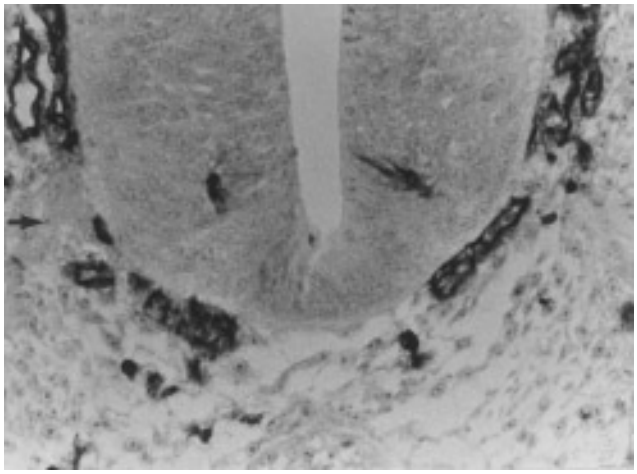

FIG. 5. Floor plate region of a chick–quail chimera (HH-stage 23). The donor NT has been perfectly integrated into the host embryo. The developing Schwann cells around the ventral root (arrow) are of chick origin and hence lack the nuclear marker characteristic for the quail host. Note the tips of ventral sprouts of host, i.e., quail origin, directed toward the central canal of the donor, i.e., chick, neural tube. Their somewhat fuzzy appearance corresponds to the abundant filopodia shown in Fig. 4.

angioblasts and sprouts, then amounted to more than 70% of the dorsal plus intermediate population, consisting of isolated angioblasts only. This was quite in contrast to the younger stages, when the ventral population was less than 10% of the combined dorsal and intermediate groups.

Craniocaudal distribution. No reference structure could be defined in craniocaudal direction. Therefore, we used the relative intercellular distances for analyzing the axial distribution (Fig. 8). The first angioblasts in the dorsal NT were spaced at irregular intervals, ranging from 0 to 150 μm, but also intercellular gaps of more than 300 μm were seen. In the intermediate third, a tendency toward a unimodal distribution between 30 and 100 μm was observed. Only four ventral sprouts were found in one HH-stage 20 embryo.

During HH-stages 21 and 22, the increasing number of angioblasts followed the same pattern: in the dorsal third, angioblasts were found in random, mutually independent positions, and large gaps were less frequent. In the intermediate third, a more regular distribution was recognized, which was significantly different from the Poisson case ($P < 0.05$), since intercellular distances below 25 μm were less frequent than could be expected. The few ventral sprouts were randomly distributed.

At HH-stages 23 and 24, the dorsal distribution still conformed with a purely random pattern, whereas in the intermediate and ventral thirds a more regular distribution was established. It was interesting to note that in the intermediate third a twofold increased frequency of large interangioblastic distances was observed. The diminished frequency of small intercellular distances was an indication of focal disappearance of angioblasts from this compartment.

DISCUSSION

We have analyzed the distribution of angioblastic cells within the cervical neural tube of quail embryos (HH-stages 19 through 24). Our observation that the first intraneural angioblasts invade the dorsal third before ventral sprouts have entered the neural tube is new and may settle the contradictory opinions on NT vascularization present in the literature (Feeney and Watterson, 1946; Strong, 1961; Noden, 1991). Using chick–quail chimeras we have proven that invasive angioblasts and sprouts originate exclusively from the mesenchyme. In addition to the results of 3-D reconstruction and CLSM morphology, the quantitative analysis of angioblast position leads to the conclusion that these cells initially are randomly distributed in the axial direction. A more regular pattern is observed later in the ventral third of neural tube, where the first perfused capillaries are formed.

In this study, we avoid the terms ''vasculogenesis,'' i.e., *in situ* differentiation vs ''angiogenesis,'' i.e., sprouting (Risau, 1991; Flamme *et al.*, 1995), because they fail to fully describe the variety of observed phenomena. As we show here, blood vessel formation in the neural ectoderm involves at least two distinct processes, but not intraneural differentiation of angioblasts. We therefore favor the more general and linguistically more correct distinction of Sherer (1991) between angioblastic and angiotrophic growth (Brand-Saberi *et al.*, 1995; Wilting *et al.*, 1995a), which better fits the multiple aspects of endothelial differentiation, migration, and assembly (Noden, 1991; Kurz *et al.*, 1994, 1995). A detailed discussion can be found in the review by Wilting *et al.* (1995b). In this terminology, we observe angiotrophic growth in the NT, by the combined action of migrating and of sprouting angioblasts. Only for the sake of clarity, and to underline their being connected to perfused vessels, we name the latter sprouting endothelial cells.

Angioblasts Migrate into the Dorsal Neural Tube Prior to Ventral Sprout Formation

This was observed constantly at HH-stage 19 in the cervical region. Looking at the NT at the leg level in older HH-stages (23, 24), the same sequence of dorsal immigration and ventral penetration was seen (data not shown). Intraneural blood vessel formation appears to follow the well-known craniocaudal sequence of differentiation like somite formation or neural crest cell emigration. It is remarkable that the neural tube is invaded first dorsally, where perfused vessels are rare in the surrounding mesenchyme. Correspondingly, the ventral penetration of endothelial sprouts originates from the primitive arterial tracts rarely before HH-stage 21, although the PATs are perfused vessels since HH-stage 16, and in close contact with the NT basal lamina. Probably there are differences in the composition or texture of the basal lamina, which might explain the varying restric-

tions on penetration of mesenchymal cells into the ectodermal neural tube.

Neural crest cells have largely emigrated from the cervical neural tube at HH-stage 18, and angioblasts start invading the dorsal neural tube at HH-stage 19, as we have shown here (cf. Figs. 1A, 2A, and 8). As LeDouarin (1982) states, the dorsal neural tube is not surrounded by a continous basement membrane when neural crest migration begins (cf. Poelmann *et al.*, 1990). It seems likely that the basement membrane remains permeable also in the opposite direction for angioblasts, which enter the NT. This is supported by our observation that angioblasts inside the NT, in contrast to those outside it, may have incorporated extracellular matrix components like laminin and fibronectin (not shown). Inclusion of matrix components was observed earlier for neural crest cells (Poelmann *et al.*, 1990), indicating a similar behavior for these two different cell lines with extended migratory capability. A possible site of angioblast invasion is the developing dorsal root, where angioblasts prefer to reside (Figs. 1B and 8), and where cell shapes such as in Figs. 6B and 6C can be observed. We therefore propose that migrating angioblasts first enter the NT in the dorsolateral region using migratory pathways similar to those used by neural crest cells.

Angioblasts Appear Initially Asymmetrically

The differences in the number of dorsal angioblasts on either side of the NT indicate that invasion is a focal, bilaterally independent process: once a cell has managed to enter the NT, this could facilitate the entrance of additional angioblasts. Whether angioblasts proliferate in the NT remains to be shown. When averaged over four embryos, angioblast numbers did not show significant differences during the first day of NT vascularization. We therefore take the lateral differences as a further sign of the random character of angioblast migration and invasion.

Sprouting Endothelial Cells Project Long Filopodia for Establishing Cellular Contacts

With the CLSM we have shown that the leading cells of intraneural vascular sprouts possess filopodia with varicosities (Figs. 3 and 4). We demonstrate for the first time the enormous number and length, and the peculiar orientation of these cell processes, which we found exclusively in the neural epithelium. Tips of filopodia were seen oriented in almost all directions, but with a preference for the ependymal surface and a complete avoidance of the developing anterior motor column. Again, this may be a sign for an intrinsically random projection of filopodia by angioblasts, possibly modified by extrinsic factors. Cell adhesion molecules such as HNK-1 and neuropilin (Takagi *et al.*, 1995), and matrix components like hyaluronan (Feinberg and Beebe, 1983; Poelmann *et al.*, 1990; Eggli *et al.*, 1992; Eggli and Graber, 1995) and vitronectin (Seiffert *et al.*, 1995), have to be considered. First results show that in the motor column, where blood vessels appear rather late (beyond HH-stage 29), HNK-1 expression is very low (data not shown). HNK-1 levels were higher in the ependymal region, where we saw tips of filopodia reaching the ependymal surface, interposed between the tight junctions of neuroblasts. An intense HNK-1 signal was seen in the region of the dorsal root, corresponding to an abundance of angioblasts in older stages.

Dorsal Angioblasts Traverse the Neural Tube Ventrad and Contribute to Intraneural Capillaries

The dorsal and intermediate NT third are populated with singly migrating angioblasts until HH-stage 22, with the majority of cells located near the dorsal root (Fig. 8). Most of the population then migrate ventrad and are found interposed between sprouts or associated with developing vessels (Figs. 2–4). Even after HH-stage 24, dorsal angioblasts were observed (Fig. 8), which most probably continue to invade the NT from outside. The internal course of dorsoventral migration could be explained with the varying mechanical resistance of the neuroepithelium due to increased density of nuclei and mitoses in the ependymal layer. In addition, a high hyaluronan concentration around mitotic cells (cf. Poelmann *et al.*, 1990) could prevent angioblast immigration into the ependymal layer (Feinberg and Beebe, 1983), whereas hyaluronan degradation products could facilitate migration and assembly of blood vessels (cf. West *et al.*, 1985) in the periependymal region, where most angioblastic cells concentrate (Fig. 7) and where the first extensive intraneural plexus forms (Camosso *et al.*, 1976). As a quite different process, cell death in the neuroepithelium at HH-stage 17 and 18 (Homma *et al.*, 1994) could open paths not only for growing axons but also for migrating angioblasts.

FIG. 6. Angioblasts in chick–quail chimeras (HH-stage 23, at leg level). Neural tube and dorsal root ganglia (G) are of chick origin and hence lack the nuclear marker characteristic for the quail host. (A) An isolated angioblast is located near the entrance of the left dorsal root (arrow). On the right side, only a minute profile near the dorsal root entrance can be detected. Note the avascular DRG, surrounded by its own vascular plexus. (B) In a section 10 μm caudal to A, the right ventral QH1-positive cell can be clearly identified as belonging to a sprout. The right dorsal angioblast is sectioned in the region of the nucleus. (C) In a section 10 μm caudal to B, two or three cell processes of the sprout can be seen. The dorsal angioblast appears flat, with processes corresponding to lamellipodia. The immediate proximity to the dorsal root is suggestive of the cell entering the NT together with the central neural crest cell processes (arrow).

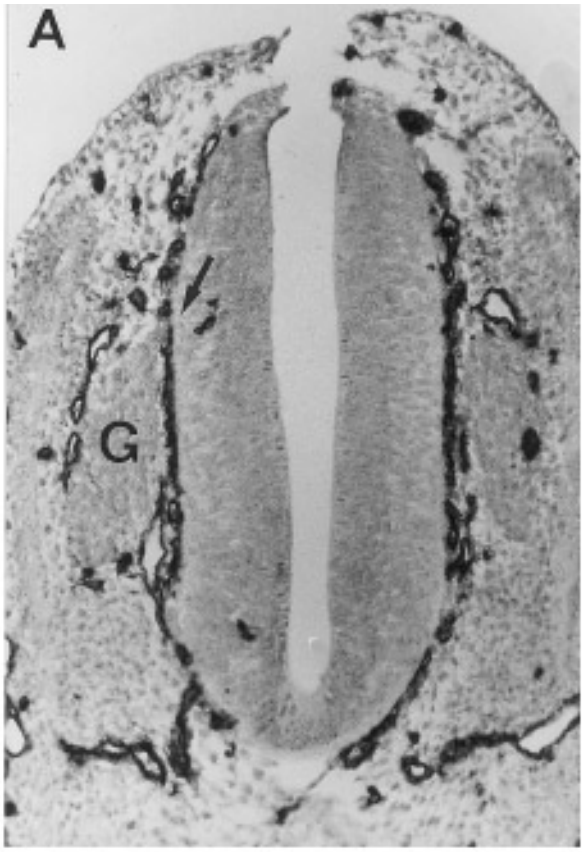
A
G

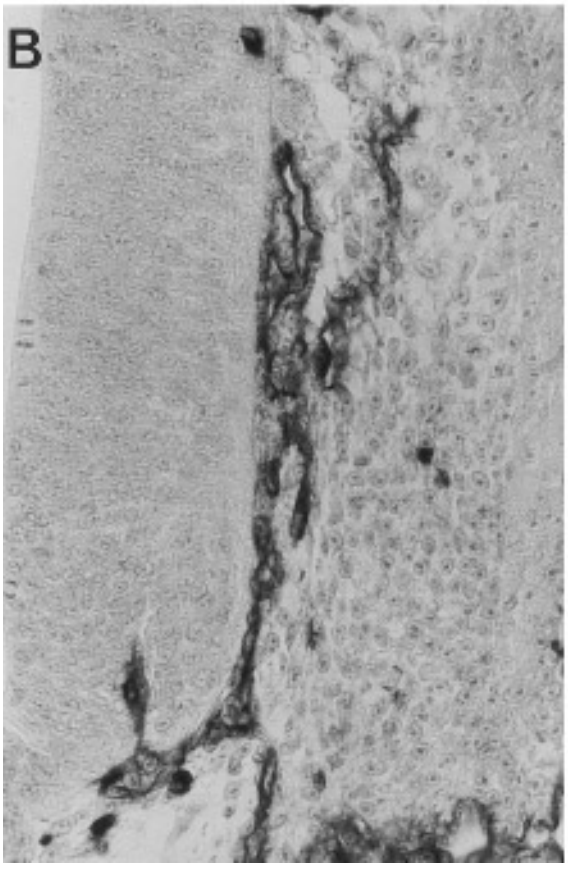
B

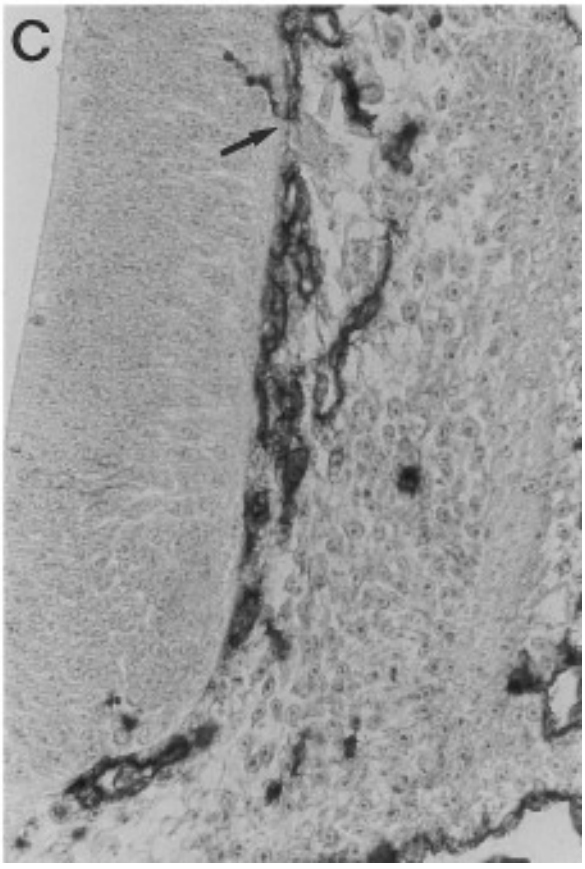
C

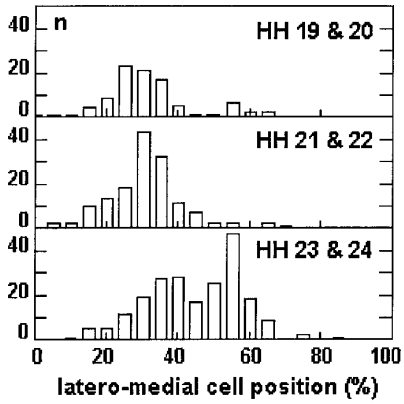

FIG. 7. Lateromedial distribution of angioblasts in the NT during the fourth day of incubation. The frequency is given over a scale of relative distance from the basal lamina (0%: lateral) to the surface of the central canal (100%: medial). A shift during development from the outer third (mantle layer) toward the middle third is obvious; the inner third (ependymal layer) is rarely occupied.

Angioblasts and Segmental Pattern

In view of the angiogenic potential of all somite compartments (Huang *et al.*, 1994; Wilting *et al.*, 1995a; Christ and Ordahl, 1995), a somitic origin of the dorsal angioblasts appears possible. Whether the early dorsal angioblasts migrated directly from the somite or whether they had been integrated in, e.g., the perineural vascular plexus previously, and then detached from it, remains open. Preliminary results from older stages with DiI-LDL/QH1 double labeling (cf. Brand-Saberi *et al.*, 1995; Brand-Saberi, personal communication) are not in favor of the second possibility.

Our findings support the view of an internally completely unsegmented neural tube (Lim *et al.*, 1991) caudal to the cervical level. They do not, however, oppose a segmental origin of dorsal angioblasts. The ventral sprouts arise in a similarly unordered fashion, which is in contrast to the regular (though not segmentally organized) pattern of the later, perfused intraneural vessels (Camosso *et al.*, 1976, Kurz *et al.*, 1993). We suppose that perfusion modifies the early patterns described here, as suggested by Noden (1991) and Clark (1991) for the cardiovascular system in general. The influence of segmentation may be different, however, in the region of rhombomeres. Preliminary results indicate that dorsal invasive angioblasts were considerably less frequent in the brain stem. Ventral sprouts consequently were the single source of intraneural vessels there, but were not arranged in a recognizable segmental pattern.

Chick–Quail Chimerization Demonstrates the Exclusive Mesodermal Origin of Intraneural Angioblasts

Following replacement of quail neural tube with chick NT, the same pattern of individual angioblasts and ventral sprouts was observed as in normal quail embryos (Figs. 5 and 6). All blood vessels consisted exclusively of QH1-positive, i.e., host-derived invasive endothelial cells. This was supported by the *vice versa* experiment, where no QH1-positive structures were found inside the grafted quail NT (data not shown). Our findings are in some contrast to Noden (1991), who stated that "invasive angioblasts do not enter the neural epithelium," and who claimed that sprouting occurs at precisely specified times and locations (in the rostral hindbrain). A possible explanation for this discrepancy is that we inserted a chick NT into a quail host, whereas Noden transplanted quail tissue into chick hosts. In a minor series of grafting quail somites into chick hosts (data not shown), we also did not see invasive angioblasts, although extraneural chimeric blood vessels were seen in the dorsal and contralateral PNVP. From this peculiar behavior we conclude that an intact tissue environment around the dorsolateral NT and the somite is a prerequisite for invasion to take place.

Alternatively, a neural crest origin of endothelial cells could be possible but seems unlikely in view of the current opinion that neural crest cells can contribute to vessel walls, but never to their endothelial lining (LeDouarin, 1982; Noden, 1983, 1991). This possibility was ruled out by the *vice versa* chimerization (not shown), in which we did not see QH1-positive structures inside the transplanted quail NT. In addition, our own double labeling studies with the neural crest cell marker HNK-1, and QH1, showed clearly distinct signals on different cell populations in all neuroectodermal tissues and thus confirm this view (data not shown).

Monocytes/Macrophages Are Not Present in the HH-Stage 19 to 24 Neural Tube

Leukocytes are practically absent from the blood in avian embryos before Incubation Day 6, and circulating monocytes are observed first a short time before hatching (Lemez, 1979). Nevertheless, we checked for the occurence of leukocyte markers in additional samples of the same specimens described before. No unspecific esterase or MPX activity was seen in any part of the NT. Very rarely, MPX-positive cells could be located in the surrounding mesenchyme, but never close to the NT. Similarly, esterase-positive cells were occasionally detected, but always far from the NT (data not shown). Two additional monoclonal antibodies (donation of Dr. Suzan Jeurissen, Lelystad) were used for identifying leukocytes in unfixed chicken cryosections of HH-stages 19, 22, and 24. The antibody CVI-ChNL-68.1 labels cells of the monocyte/macrophage lineage (Jeurissen *et al.*, 1988, 1992), whereas HIS-C7 detects the CD45 chicken common leukocyte antigen. Single cells were detected exclusively in mesenchymal tissues (data not shown). We therefore conclude that all intraneural QH1-positive cells up to HH-stage 24 are endothelial cells and their precursors, and not leukocytes or macrophages.

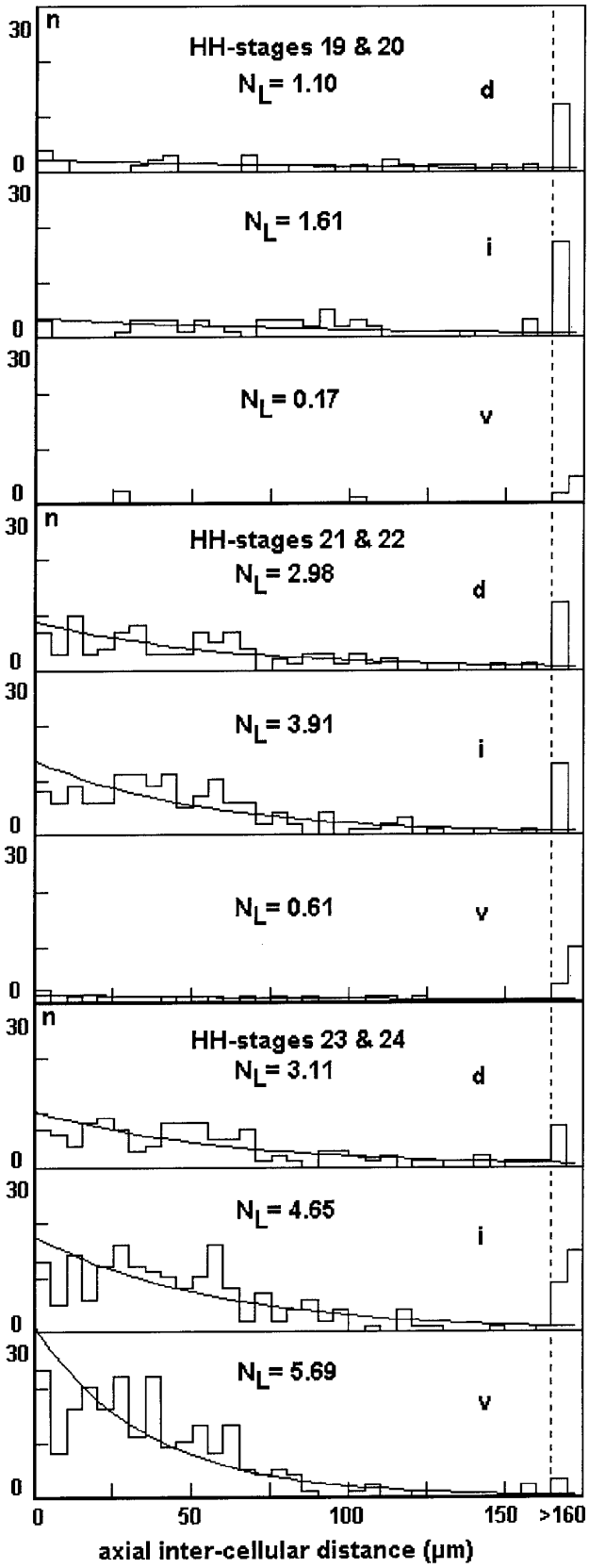

Vascular Endothelial Growth Factor and Intraneural Vascular Pattern

Vascular endothelial growth factor (VEGF) is produced in the ependymal layer as reported by Breier *et al.* (1992). VEGF essentially is an endothelial cell-specific mitogen (Leung *et al.*, 1989; Wilting *et al.*, 1993; Millauer *et al.*, 1993; Kurz *et al.*, 1994, 1995; Dumont *et al.*, 1995), and it is difficult to see how it defines the location of invasion or the internal course of blood vessels within the NT. In particular, the report by Flamme *et al.* (1995) suggests that a majority of intraneural QH1-positive cells express the VEGF receptor *flk-1*. This does not explain, however, why the proposed source of VEGF, the ependymal layer—and the motor column—is strictly avoided. We would like to stress the role of VEGF as a mitogenic stimulus for all endothelial cells and their precursors (Kurz *et al.*, 1995). On the other hand, it has been shown recently that in mice the VEGF receptor *flt-1* (Fong *et al.*, 1995) and the *Tie-1* and *Tie-2* receptors (Sato *et al.*, 1995) are essential for correct endothelial assembly. It remains to be shown if, and eventually how, these mechanisms contribute to intraneural blood vessel patterning.

Conclusions

One should be aware of the difference between the vascular pattern and the perfusion pattern, the latter being more

FIG. 8. Dorsoventral and craniocaudal distribution of angioblasts in the neural tube. Three diagrams show the intercellular distances in the three age groups (four embryos each, left and right sides combined). Distributions for the dorsal, d, intermediate, i, and ventral third, v, are shown separately, with the ordinate, n, representing the number of observations in 5-μm intervals. The abscissa is linear up to 160 μm; two units beyond the dashed line correspond to the largest ranges of 160 to 320 μm, and of more than 320 μm, respectively. N_L indicates the mean number of angioblasts or sprouts per 100-μm NT length. For the observed mean intercellular distances, d, the probability densities of Poisson distributed distances, x, given by $(e^{-x/d})/d$, are shown to indicate the expected distance distribution in case of absolute independence of the cells (continuous line). The intermediate third is the most populated part until HH-stage 22, when comparatively few sprouts in the ventral region have formed. Note that at HH-stages 23 and 24, almost 10 times as many cells per 100 μm are found in the ventral third, compared to HH-stages 21 and 22. The observed distributions comply with the assumption of axial independent random position for all regions in the youngest embryos, but only for the dorsal and ventral third in HH-stages 21 and 22, and the dorsal third of the oldest embryos. In the intermediate region of HH-stages 21 and 22, and in the intermediate and ventral region of HH-stages 23 and 24, the observed distance distribution has become significantly different from a Poisson distribution ($P \leqslant 0.05$). This is due to a loss of short intercellular distances and most likely corresponds to fusion processes of angioblasts with sprouts or of neighboring sprouts with each other.

regular than the former. We support the view of Noden (1991) that one has to distinguish the structural from the functional properties during embryonic blood vessel formation. We extend his view that embryonic angioblasts are highly invasive, moving in virtually every direction not only throughout mesenchymal tissues, but also inside most of the neural tube. Cells of the neural tube impose constraints upon angioblast and sprout distribution. In summary, angioblastic cells are not told where to go, they are told where not to go. This is the most effective way to supply the vast majority of tissues with blood vessels in a rapidly growing organism.

ACKNOWLEDGMENTS

We thank Dr. K. Sandau for his critical remarks and support of the statistical evaluation. The technical assistance of L. Koschny and M. Schüttoff and the discussions with Drs. B. Brand-Saberi and J. Wilting are gratefully acknowledged. We thank Dr. S. Jeurissen for donating chick leukocyte antibodies. Work reported here was supported by grants of the Deutsche Forschungsgemeinschaft CH44/9-2 (B.C.) and of the Swiss National Science Foundation 31-36012-92 (P.S.E.).

REFERENCES

Brand-Saberi, B., Seifert, R., Grim, M., Wilting, J., Kühlewein, M., and Christ, B. (1995). Blood vessel formation in the avian limb bud involves angioblastic and angiotrophic growth. *Dev. Dyn.* **202,** 181–194.

Breier, G., Albrecht, U., Sterrer, S., and Risau, W. (1992). Expression of vascular endothelial growth factor during embryonic angiogenesis and endothelial cell differentiation. *Development* **114,** 521–532.

Camosso, M. E., Roncalli, L., and Ambrosi, G. (1976). Vascular pattern in the chick spinal cord in normal and experimentally modified development. *Acta Anat.* **95,** 349–367.

Christ, B., Poelmann, R. E., Mentink, M. M. T., and Gittenberger-de Groot, A. C. (1990). Vascular endothelial cells migrate centripetally within embryonic arteries. *Anat. Embryol.* **181,** 333–339.

Christ, B., and Ordahl, C. P. (1995). Early stages of chick somite development. *Anat. Embryol.* **191,** 381–396.

Clark, E. B. (1991). Functional characteristics of the embryonic circulation. *In* ''The Development of the Vascular System'' (R. N. Feinberg, G. K. Sherer, and R. Auerbach, Eds.), pp. 125–135. Issues Biomed., Vol. 14. Karger, Basel.

Connolly, D. T., Heuvelman, D., Nelson, R., Olander, J. V., Eppler, B. L., Delfino, J. J., Siegel, N. R., Leimgruber, R. M., and Feder, J. (1989). Tumor vascular permeability factor stimulates endothelial cell growth and angiogenesis. *J. Clin. Invest.* **84,** 1470–1478.

Dumont, D. J., Fong, G.-H., Puri, M. C., Gradwohl, G., Alitalo, K., and Breitman, M. L. (1995). Vascularization of the mouse embryo: A study of flk-1, tek, tie, and vascular endothelial growth factor expression during development. *Dev. Dyn.* **203,** 80–92.

Eggli, P. S., Lucocq, J., Ott, P., Graber, W., and van der Zypen, E. (1992). Ultrastructural localization of hyaluronan in myelin sheaths of the rat central and rat and human peripheral nervous systems using hyaluronan-binding protein-gold and link protein-gold. *Neuroscience* **48,** 737–744.

Eggli, P. S., and Graber, W. (1995). Association of hyaluronan with rat vascular endothelial and smooth muscle cells. *J. Histochem. Cytochem.* **43/7,** 689–697.

Feeney, J. F., Jr., and Watterson, R. L. (1946). The development of the vascular pattern within the walls of central nervous system of the chick embryo. *J. Morphol.* **78,** 231–304.

Feinberg, R. N., and Beebe, D. C. (1983). Hyaluronate in vasculogenesis. *Science* **220,** 1177–1179.

Flamme, I., Breier, G., and Risau, W. (1995). Vascular endothelial growth factor (VEGF) and VEGF receptor 2 (flk-1) are expressed during vasculogenesis and vascular differentiation in the quail embryo. *Dev. Biol.* **169,** 699–712.

Fong, G.-H., Rossant, J., Gertsenstein, M., and Breitman, M. L. (1995). Role of the Flt-1 receptor tyrosine kinase in regulating the assembly of vascular endothelium. *Nature* **376,** 66–70.

Hamburger, V., and Hamilton, N. (1951). A series of normal stages in the development of the chick embryo. *J. Morphol.* **88,** 49–92.

Homma, S., Yaginuma, H., and Oppenheim, R. W. (1994). Programmed cell death during the earliest stages of spinal cord development in the chick embryo: A possible means of early phenotypic selection. *J. Comp. Neurol.* **345,** 377–395.

Huang, R., Zhi, Q., Wilting, J., and Christ, B. (1994). The fate of somitocoele cells in avian embryos. *Anat. Embryol.* **190,** 243–250.

Jeurissen, S. H. M., Janse, E. M., Koch, G., and de Boer, G. F. (1988). The monoclonal antibody CVI-ChNL-68.1 recognizes cells of the monocyte-macrophage lineage in chicken. *Dev. Comp. Immunol.* **12,** 855–864.

Jeurissen, S. H. M., Claassen, E., and Janse, E. M. (1992). Histological and functional differentiation of non-lymphoid cells in the chicken spleen. *Immunology* **77,** 75–80.

Kurz, H., Pohland, C., Wilting, J., and Christ, B. (1993). Pattern formation of blood vessels in the neural tube of avian embryos. *Ann. Anat.* **175** (Suppl.), 142–143.

Kurz, H., Wilting, J., and Christ, B. (1994). Multivariate characterization of blood vessel morphogenesis in the avian chorioallantoic membrane (CAM). *In* ''Fractals in Biology and Medicine'' (G. E. Losa, T. F. Nonnenmacher, and E. R. Weibel, Eds.), pp. 132–140. Birkhäuser, Boston.

Kurz, H., Ambrosy, S., Wilting, J., Marmé, D., and Christ, B. (1995). The proliferation pattern of capillary endothelial cells in chorioallantoic membrane development indicates local growth control, which is counteracted by vascular endothelial growth factor application. *Dev. Dyn.* **203,** 174–186.

Le Douarin, N. M. (1982). The Neural Crest. Cambridge Univ. Press, Cambridge.

Lemez, L. (1979). Quantitative data on haemocytoblasts, granulocytes, lymphocytes and monocytes in circulating blood of chick embryos. *Folia biologica (Praha)* **25,** 319–320.

Leung, D. W., Cachianes, G., Kuang, W. J., Goeddel, D. V., and Ferrara, N. (1989). Vascular endothelial growth factor is a secreted angiogenic mitogen. *Science* **246,** 1306–1309.

Lim, T.-M., Jaques, K. F., Stern, C., and Keynes, R. J. (1991). An evaluation of myelomeres and segmentation of the chick embryo spinal cord. *Development* **113,** 227–238.

Millauer, B., Wizigmann-Voos, S., Schnürch, H., Martinez, R., Moller, N. P. H., Risau, W., and Ullrich, A. (1993). High affinity VEGF binding and developmental expression suggest flk-1 as a

major regulator of vasculogenesis and angiogenesis. *Cell* **72,** 835–846.

Noden, D. M. (1983). The role of the neural crest in patterning of avian cranial skeletal, connective, and muscle tissues. *Dev. Biol.* **96,** 144–165.

Noden, D. M. (1991). Development of craniofacial blood vessels. *In* ''The Development of the Vascular System'' (R. N. Feinberg, G. K. Sherer, and R. Auerbach, Eds.), pp. 1–23. Issues Biomed. Vol. 14. Karger, Basel.

Pardanaud, L., and Dieterlen-Liévre, F. (1993). Emergence of endothelial and hemopoietic cells in the avian embryo. *Anat. Embryol.* **187,** 107–114.

Pardanaud, L., Altmann, C., Kitos, P., Dieterlen-Liévre F., and Buck, C. A. (1987). Vasculogenesis in the early quail blastodisc as studied with a monoclonal antibody recognizing endothelial cells. *Development* **100,** 339–349.

Poelmann, R. E., Gittenberger-de Groot, A. C., Mentink, M. M. T., Delpech, B., Girard, N., and Christ, B. (1990). The extracellular matrix during neural crest formation and migration in rat embryos. *Anat. Embryol.* **182,** 29–39.

Risau, W. (1991). Vasculogenesis, angiogenesis and endothelial differentiation during embryonic development. *In* ''The Development of the Vascular System'' (R. N. Feinberg, G. K. Sherer, and R. Auerbach, Eds.), pp. 58–68. Issues Biomed. Vol. 14. Karger, Basel.

Sato, T. N., Tozawa, Y., Deutsch, U., Wolburg-Buchholz, K., Fujiwara, Y., Gendron-Maguire, M., Gridley, T., Wolburg, H., Risau, W., and Qin, Y. (1995) Distinct roles of the receptor tyrosine kinases Tie-1 and Tie-2 in blood vessel formation. *Nature* **376,** 70–74.

Seiffert, D., Iruela-Arispe, M. L., Sage, E. H., and Loskutoff, D. J. (1995) Distribution of vitronectin mRNA during murine development. *Dev. Dyn.* **203,** 71–79.

Sherer, G. K. (1991). Vasculogenic mechanisms and epithelio-mesenchymal specifity in endodermal organs. *In* ''The Development of the Vascular System'' (R. N. Feinberg, G. K. Sherer, and R. Auerbach, Eds.), pp. 37–57. Issues Biomed. Vol. 14. Karger, Basel.

Sterzi, G. (1904). Die Blutgefäße des Rückenmarks. Untersuchungen über ihre vergleichende Anatomie und Entwicklungsgeschichte. *Anat. Hefte* **24,** 1–364.

Stoyan, D., and Stoyan, H. (1994). ''Fractals, Random Shapes, and Point Fields.'' Wiley, New York.

Strong, L. H. (1961). The first appearance of vessels within the spinal cord of the mammal: Their developing patterns as far as partial formation of the dorsal septum. *Acta Anat.* **44,** 80–108.

Strong, L. H., and Winston, M. (1957). The development of the arteries of the spinal medulla of the rabbit, from their beginning through the formation of the posterior cordal septum. *Anat. Rec.* **127,** 374.

Takagi, S., Kasuya, Y., Shimizu, M., Matsuuura, T., Tsuboi, M., Kawakami, A., and Fujisawa, H. (1995). Expression of a cell adhesion molecule, neuropilin, in the developing chick nervous system. *Dev. Biol.* **170,** 207–222.

West, D. C., Hampson, I. N., Arnold, F., and Kumar, S. (1985). Angiogenesis induced by degradation products of hyaluronic acid. *Science* **228,** 1324–1326.

Wilting, J., Christ, B., Bokeloh, M., and Weich, HA. (1993). *In vivo* effects of vascular endothelial growth factor on the chicken chorioallantoic membrane. *Cell Tissue Res.* **274,** 163–172.

Wilting, J., Brand-Saberi, B., Huang, R., Zhi, Q., Köntges, G., Ordahl, C., and Christ, B. (1995a). Angiogenic potential of the avian somite. *Dev. Dyn.* **202,** 165–171.

Wilting, J., Brand-Saberi, B., Kurz, H., and Christ, B. (1995b). Development of the embryonic vascular system. *Cell. Mol. Biol. Res.*, **41** (4), in press.

Received for publication August 7, 1995
Accepted September 26, 1995